



## **Flexural stiffness factors for stability design of stainless steel planar frames**

Yanfei Shen<sup>1</sup>, Rolando Chacón<sup>2</sup>

### **Abstract**

The Direct Analysis Method is the primary method for the stability design of carbon steel frames in AISC 360-16. The method refers to a second-order elastic analysis performed on members whose tangent stiffness moduli are reduced using adequate factors. The aim of this research is to provide a set of stiffness reduction factor formulation for the stability design of the particular case of stainless steel frames. The proposed stiffness reduction factor is aligned to AISC 360-16 and it is aimed at facilitating greater and more efficient use of stainless steel, whose material nonlinearity must be accounted for in design. The focus of this research is the development of flexural stiffness reduction factor formulation for the in-plane stability design of stainless steel elements and frames with cold-formed square hollow section and rectangular hollow sections. A beam-column stiffness reduction factor accounting for the deleterious influence of material non-linearity, residual stresses and member out-of-straightness is proposed. The use of a second-order elastic analysis coupled with the proposed reduction factor eliminates the need for member buckling strength checks and thus, only cross-sectional strength checks are required. For the case of beam-columns, two types of reduction factors are developed: analytical and approximate. The analytical expression presumes knowing the maximum internal second order moment within a member. It is developed by means of extending the formulations for evaluating the elastic second order effects to the inelastic range. The approximate expression is of considerable usefulness since in practical design, the second order moment is not known in advance. As a result, an approximate expression of the reduction factor, which is assumed to be a function of relevant variables, is proposed by fitting variables to the analytically determined expression. For the purpose of developing this approximate expression, column flexural stiffness reduction factors as well as and beam flexural stiffness reduction factors are derived from stainless steel column strength curves and from the moment-curvature relationship, respectively.

### **1. Introduction**

The use of a second-order elastic analysis together with an appropriate stiffness reduction represents a straightforward alternative to determine internal forces and moments for ultimate limit state design checks. This method captures second order effects at system and member levels and

---

<sup>1</sup> Lecturer, Wuyi University, China, <shenyanfei@wyu.edu.cn>

<sup>2</sup> Associate Professor, Technical University of Catalonia, Spain, <rolando.chacon@upc.edu>

may be adopted using reduced stiffness to account for the influence of material nonlinearity and residual stresses. For second-order elastic analysis coupled with stiffness reduction, the initial member out-of-straightness ( $\delta/L$ ) can be accounted for by geometrically modelling out-of-straightness directly, by applying equivalent horizontal loads appropriately, by reducing stiffness implicitly using reduction factors or by checking buckling resistance of individual members.

A representative example of the use of a second-order elastic analysis together with stiffness reduction is the Direct Analysis Method (DM). DM first appeared in the 2005 version of the Specification for Structural Steel Buildings (ANSI/AISC 2005) as an alternative to the Effective Length Method (ELM) for frame stability design. It was subsequently upgraded and reorganized (ANSI/AISC 2010, 2016) as the primary method for frame stability design (ELM was moved to Appendix 7). When compared to the effective length method, a significant advantage of second-order elastic analysis with stiffness reduction is that it eliminates the need of calculating effective length of the column. Accurate estimations of the effective length factors are rather difficult for geometrically irregular frames. Another advantage of the method is that it provides more accurate internal moments, which is a great concern for the design of connections. In most cases, second-order elastic analysis together with stiffness reduction provides enhanced representations of internal moments for ultimate limit states verifications (White et al. 2006, Kucukler et al. 2016) since values are closer to the values obtained by second-order inelastic analysis.

AISC Design Guide 27, Structural Stainless Steel (Baddoo 2013) provides guidance for the design of stainless steels structures (Baddoo and Francis 2014). It states that geometrically nonlinear analysis with stiffness reduction can be a reference method to stability design of stainless steel frames provided that the member strengths are determined in accordance to AISC (Baddoo 2013). Presently, the Direct Analysis Method in ANSI/AISC (2016) conservatively adopts a maximum allowable out-of-plumbness ( $\Delta/h$ ) of 0.002 in order to account for the initial global sway imperfection of the system. The influence of member out-of-straightness ( $\delta/L$ ) is considered by member buckling strength check where the column is taken as pinned at both ends (the effective length factor is equal to 1). For frames with intermediate or stocky columns, a general flexural stiffness reduction factor  $0.8\tau_b$  is suggested to account for inelastic softening prior to the members reaching their design strength. The bending stiffness of members with an axial load in excess of  $0.5P_y$  ( $P_y$  is cross-section yield strength) is reduced by the factor  $\tau_b$  derived from CRC column strength curve, to account for the influence of partial yielding accentuated by the presence of residual stresses (White et al. 2013). The factor 0.8, originally proposed by Surovek-Maleck and White (2004<sup>a,b</sup>), accounts for additional softening under combined axial loading and bending moments.

Although calibration studies have shown that the flexural stiffness reduction factor  $0.8\tau_b$  is appropriate to stability design of carbon steel beam-columns and frames, it may not be appropriate to the stainless steel counterparts. Stainless steel presents a nonlinear constitutive equation and column buckling curves of stainless steel differ from those derived for carbon steel. Therefore, to use stiffness reduction factors for the stability design of stainless steel members and frames, an appropriate stiffness reduction factor is needed.

This paper depicts the derivation of column flexural stiffness reduction factor ( $\tau_N$ ), beam flexural stiffness reduction factor ( $\tau_M$ ), and the development and verification of both analytical and

approximate beam-column stiffness reduction factor ( $\tau_{MN}$ ) for stainless steel. In addition, for the specific case of slender cross-sections, these factors are appropriately reduced with a corresponding  $\rho$  that accounts for the influence of local buckling.

## 2. Literature review

Previous research on determination of beam-column flexural stiffness reduction factor is available for carbon steel. Kucukler et al. (2014,2016), Kucukler and Gardner (2018,2019<sup>a</sup>,2019<sup>b</sup>) developed a function of beam-column flexural stiffness reduction factor for using second-order elastic analysis for the design of in-plane carbon steel beam-columns and frames with compact sections. The function includes as parameters: first order maximum axial force, first order maximum bending moment, column flexural stiffness reduction factor, beam flexural stiffness reduction factor, and a moment gradient factor  $C_m$ . In the context of that research, the column stiffness reduction factor was derived from European column buckling curves whereas beam flexural stiffness reduction factors were developed using an empirical formulation. For the proposed flexural stiffness reduction formulations, strain-hardening after achieving full plastic strength of the cross-section was not considered. The residual stresses pattern recommended by the European Convention for Construction Steelwork (ECCS) was adopted for compact I or H sections. Zubydan (2010) previously provided a methodology for estimating the flexural stiffness reduction factor for compact cross-sections subjected to combined axial loading and bending moment.

Furthermore, White et al. (2016) proposed a simple interpolation equation to represent a beam-column flexural stiffness reduction factor to be used in the stability design checks of carbon steel members and frames with I-sections. The general expression of the interpolation equation is  $\tau_{MN}(\text{White et al}) = \rho^* \tau_a(\theta/90^\circ) + \tau_{M,AISC} (1-\theta/90^\circ)$ . In this expression, the angle  $\theta$  represents the position of the current force point within a normalized interaction plot of the axial and moment strength ratios for a given cross-section. On the other hand,  $\rho^*$  accounts for local buckling effects,  $\tau_a$  is derived from column buckling curves given in ANSI/AISC (2016) and  $\tau_{M,AISC}$  is derived from lateral-torsional buckling (LTB) curves of beams given. For using second order refined plastic hinge method to frame stability design, Kim and Chen (1999) extended the column flexural stiffness reduction factor derived CRC column strength curve, to be applicable to beam-columns with compact I cross-sections.

When it comes to stainless steel, the mechanical properties of this material (e.g., high ductility, strain-hardening, an adequate behavior at high temperatures and excellent life-cycle properties) provide an alternative as a construction material for structures (Baddoo 2008, Rossi 2014). In the recent decades, a considerable amount of research has been devoted to the understanding of the structural performance of the material (Arrayago et al. 2015) and isolated stainless steel members (Gardner 2019). Nevertheless, advances related to the analysis of more complex stainless steel structures, such as frames, are recent and still scarce. Recent research on the behavior of stainless steel frames by Walport et al. (2019) show that the material nonlinearity and the corresponding degradation of stiffness affects the characteristics of the structural system, causing greater deformations and increasing second order effects. The definition of lateral stability of frames is directly affected. Furthermore, the limited use of plastic design for stainless steel frames is an obstacle for the adequate exploitation of enhanced material characteristics. In a research project developed in Spain, stainless steel frames have been studied experimentally and numerically. Arrayago et al. (2020<sup>a</sup>,2020<sup>b</sup>) deployed an experimental program on sway and non-sway stainless

steel frames (both compact and slender) subjected to vertical and horizontal loading. On the same program, Chacón et al (2020,2021) developed a set of experimental measurement and visualization techniques such as VR/AR and TLS-based imperfection analysis. Shen and Chacón (2019,2020<sup>a</sup>,2020<sup>b</sup>) developed numerical studies on isolated members and planar frames (both compact and slender) for the development of stiffness reduction factors.

### 3. Column and beam reduction factors for stainless steel rectangular hollow sections

For the purpose of developing the approximate expression of beam-column reduction factor to be used for the design and verification of stainless steel frames, a previous step consists of the development of column flexural stiffness reduction factor ( $\tau_N$ ) and beam flexural stiffness reduction factor ( $\tau_M$ ). The former is derived from stainless steel column strength curves whereas the latter from a moment-curvature relationship.

For the former case, carbon steel column flexural stiffness reduction factor  $\tau_b$ , determined by Eq. 1 and 2, is derived from Column Research Council (CRC) column strength curves. The CRC column strength curve is developed based on test results of columns with hot-rolled wide-flange I sections.  $\tau_b$  is intended to mainly account for the influence of partial yielding accentuated by the presence of residual stresses, but it may not be applicable to cold-formed RHS and SHS. This is because the distribution and magnitude of residual stresses of cold-formed RHS and SHS differs from that of hot-rolled wide-flange I sections. An expression of CRC curve (for compact sections) is given by Eq. 3 and 4.

$$\tau_b = 1 \quad \text{for } \frac{P_{r1}}{P_y} \leq 0.5 \quad (1)$$

$$\tau_b = 4 \frac{P_{r1}}{P_y} \left( 1 - \frac{P_{r1}}{P_y} \right) \quad \text{for } \frac{P_{r1}}{P_y} > 0.5 \quad (2)$$

where  $P_{r1}$  is the maximum first order internal axial force;  $P_y$  is cross-section yield strength  $P_y = A f_y$ ;  $A$  is cross-section area;  $f_y$  is 0.2% proof stress.

$$P_n = \left( 1 - \frac{\lambda_c^2}{4} \right) P_y \quad \text{for } \lambda_c \leq 1.414 \quad (3)$$

$$P_n = P_e = \frac{P_y}{\lambda_c^2} \quad \text{for } \lambda_c > 1.414 \quad (4)$$

where  $P_n$  is the nominal compressive strength of a column;  $P_n$  is equal to nominal global buckling strength for a column with compact section;  $P_e$  is elastic critical buckling strength of a member;  $\lambda_c$  is column slenderness.

A new column stiffness reduction factor ( $\tau_N$ ) for cold-formed stainless steel with RHS is developed. The factor is referred to as  $\tau_N$  and it is derived from the stainless steel column strength curve provided in Section 5.3 of AISC Design guide 27 (Eq. 5 and Eq. 6):

$$P_n = 0.5 \lambda_c^2 P_y \quad \text{for } \lambda_c \leq 1.2 \quad (5)$$

$$P_n = 0.531 P_e = \frac{0.531}{\lambda_c^2} P_y \quad \text{for } \lambda_c > 1.2 \quad (6)$$

Thus, the expression of  $\tau_N$  is given by Eq. 7 and 8.  $\tau_N$  formulation accurately accounts for the effects of residual stress, member imperfection (out-of-straightness), and spread of plasticity on

stainless steel columns. It should be noted that for the determination of  $\tau_N$  under different axial load, the nominal compressive strength  $P_n$  should be replaced by the maximum internal axial force  $P_{r1}$  under corresponding axial load.

$$\tau_N = 1 \quad \text{for } \frac{P_n}{P_y} \leq 0.37 \quad (7)$$

$$\tau_N = -2.717 \frac{P_{r1}}{P_y} \ln \frac{P_{r1}}{P_y} \quad \text{for } \frac{P_n}{P_y} > 0.37 \quad (8)$$

To account for stiffness reduction caused by local buckling and initial localized imperfection ( $\omega$ ), the resistance of the gross section is reduced through incorporating the strength reduction factor  $\rho$  ( $\rho \leq 1$ ) determined by DSM. The extended column flexural stiffness reduction factor ( $\tau_{N-\rho}$ ) formulation is given Eq. 9 and 10.

$$\tau_{N-\rho} = 1 \quad \text{for } \frac{P_{r1}}{\rho P_y} \leq 0.37 \quad (9)$$

$$\tau_{N-\rho} = -2.717 \frac{P_{r1}}{\rho P_y} \ln \frac{P_{r1}}{\rho P_y} \quad \text{for } \frac{P_{r1}}{\rho P_y} > 0.37 \quad (10)$$

For members in compression,  $\rho$  is given by Eq. 11 and Eq. 12 and considers interaction between global and local buckling.

$$\frac{P_{nl}}{P_{ns}} = \rho = 1 \quad \text{for } \lambda_l \leq 0.776 \quad (11)$$

$$\frac{P_{nl}}{P_{ns}} = \rho = \lambda_l^{-0.8} - 0.15 \lambda_l^{-1.6} \quad \text{for } \lambda_l > 0.776 \quad (12)$$

where  $\lambda_l = (P_{ne}/P_{cr1})^{0.5}$ ;  $P_{nl}$  is the nominal local buckling strength in compression;  $P_{nl}$  is equal to the nominal compressive strength ( $P_n$ ) of a column (without distortional buckling);  $P_{ne}$  is the nominal global buckling strength in compression;  $P_{cr1}$  is the elastic critical local buckling strength.

The accuracy of column flexural stiffness reduction factors ( $\tau_N$  and  $\tau_{N-\rho}$ ) for predicting compressive strength of members subjected to axial load was assessed by means of a numerical parametric study in pinned columns subjected to compressive loads with varying length. For each case, 2<sup>nd</sup>-order inelastic analysis and 2<sup>nd</sup>-order elastic analysis together with stiffness reduction  $\tau_N$  were conducted. For the case of elements prone to local buckling, shell-element based simulations were conducted as well. Fig. 1 shows the obtained results for both compact and slender sections.  $P_u$  and  $P_y$  are ultimate compressive strength and cross-section yield strength, respectively.

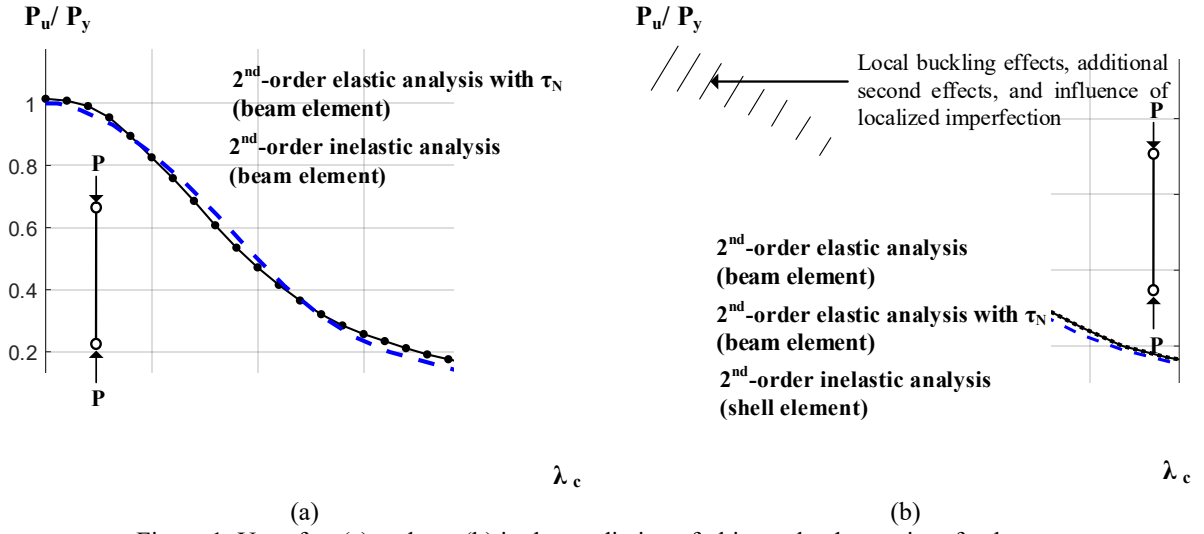


Figure 1. Use of  $\tau_N$  (a) and  $\tau_{N-p}$  (b) in the prediction of ultimate load capacity of columns

On the other hand, the bending stiffness reduction factor ( $\tau_M$ ) for in-plane beams refers to the influence of spread of plasticity through cross-section and along the member.  $\tau_M$  can be determined by the ratio of tangent flexural stiffness  $(EI)_t$  to the initial flexural stiffness  $EI$ . The adopted moment-curvature relationship prior to outer fibers yielding is based on the moment-curvature relationship for stainless steel beams with cold formed RHS and SHS proposed by Real and Mirambell (2005). It considers material non-linearity and it is fitted by an analytical expression similar to the Ramberg-Osgood equation. The moment-curvature relationship is given by Eq. 13.

$$\kappa = \frac{M_{r1}}{EI} + \left( \frac{2}{D} \left( \frac{f_y}{E} + 0.002 \right) - \frac{M_y}{EI} \right) \left( \frac{M_{r1}}{M_y} \right)^{n-1} \quad (13)$$

where  $\kappa$  is curvature;  $M_{r1}$  is the maximum internal first order moment within a member;  $EI$  is the initial flexural stiffness;  $D$  is the height of the cross-section;  $f_y$  is 0.2% proof stress;  $n$  is the coefficient in the Ramberg-Osgood equation;  $M_y$  is moment at yielding of the extreme fiber.

Based on Eq.13 and after a set of mathematical steps (largely depicted in Shen and Chacón, 2020<sup>a</sup>),  $\tau_M$  for flexural stiffness reduction before extreme fiber of the cross-section yields is given by

$$\tau_M = \left[ 1 + (n-1) \frac{0.001E}{f_y} \left( \frac{M_{r1}}{M_p} \frac{W_{pl}}{W_{el}} \right)^{n-2} \right]^{-1} \quad (14)$$

where  $M_p$  is full plastic bending moment;  $M_p = W_{pl} f_y$ ;  $W_{pl}$  and  $W_{el}$  are plastic gross section modulus and elastic gross section modulus, respectively.

For the deformation range corresponding to  $M_y < M_{r1} \leq M_p$ ,  $\tau_M$  is given by

$$\tau_M = \left[ \left( 1 - \frac{M_{r1}}{M_p} \right) \frac{1}{1 - \frac{W_{el}}{W_{pl}}} \right]^{0.9} \left[ 1 + (n-1) \frac{0.001E}{f_y} \right]^{-1} \quad (15)$$

Likewise, the extended beam flexural stiffness reduction factor ( $\tau_{M-\rho}$ ) formulation for non-compact section is given by:

$$\text{When } 0 < M_{r1} \leq \rho M_y \quad \tau_{M-\rho} = \left[ 1 + (n-1) \frac{0.001E}{f_y} \left( \frac{M_{r1}}{\rho M_p} \frac{W_{pl}}{W_{el}} \right)^{n-2} \right]^{-1} \quad (16)$$

$$\text{When } \rho M_y < M_{r1} \leq \rho M_p \quad \tau_{M-\rho} = \left[ \left( 1 - \frac{M_{r1}}{\rho M_p} \right) \frac{1}{1 - \frac{W_{el}}{W_{pl}}} \right]^{0.9} \left[ 1 + (n-1) \frac{0.001E}{f_y} \right]^{-1} \quad (17)$$

The strength reduction factor for members in bending derived by DSM is given Eq. 18 and 19.

$$\text{When } \lambda_l \leq 0.776 \quad \frac{M_{nl}}{M_{ne}} = \rho = 1 \quad (18)$$

$$\text{When } \lambda_l > 0.776 \quad \frac{M_{nl}}{M_{ne}} = \rho = \lambda_l^{-0.8} - 0.15 \lambda_l^{-1.6} \quad (19)$$

where  $\lambda_l = (M_{ne}/M_{cr1})^{0.5}$ ;  $M_{nl}$  is the nominal local buckling moment; For a beam without distortional buckling,  $M_{nl}$  is equal to the nominal flexural strength ( $M_n$ );  $M_{ne}$  is the nominal global (lateral-torsional) buckling moment;  $M_{cr1}$  is elastic critical local buckling moment.

To evaluate the ability of  $\tau_M$  capturing spread of plasticity through cross-section and along member length, beams with a wide range of cross-sections and material properties subjected to varied load cases are studied. Fig. 2(a) shows an evaluation of the flexural stiffness reduction factor ( $\tau_M$ ) for an example of the studied stainless steel beam with compact section. Fig. 2(b) shows an evaluation of the extended flexural stiffness reduction factor ( $\tau_{M-\rho}$ ) for an example of the studied stainless steel beam with slender section.

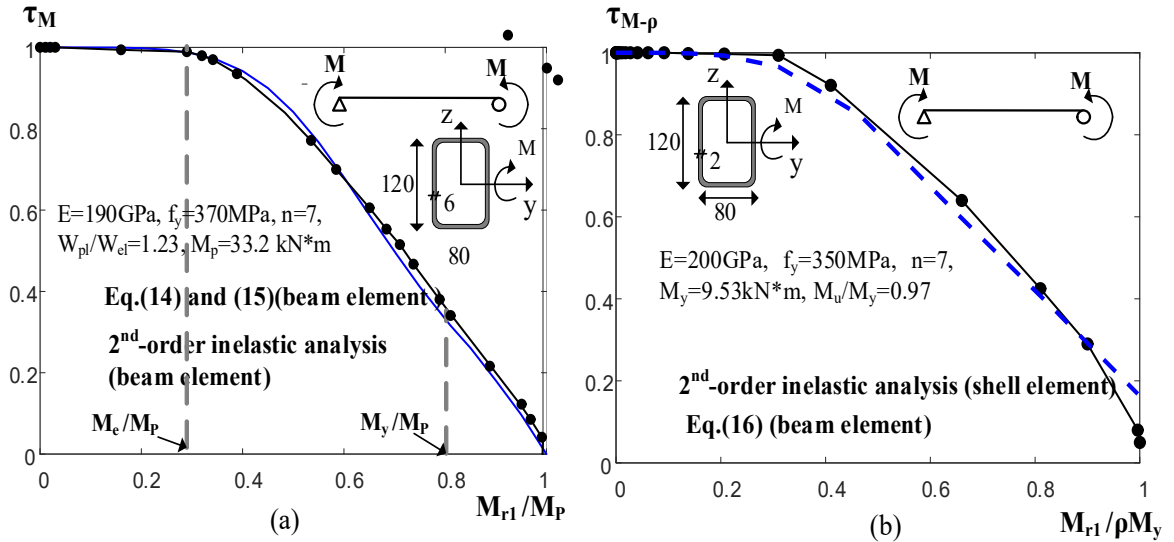


Figure 2. Comparison of flexural stiffness reduction factor ( $\tau_M$  and  $\tau_{M-\rho}$ ) determined by different methods for compact section (a) and slender section (b)

#### 4. Beam-Column for stainless steel rectangular hollow sections

Based on formulations that evaluate second order effects for elastic beam-columns, an analytical expression of stiffness reduction factor ( $\tau_{MN}$ ) for beam-columns is described. The formulations

that determine maximum internal forces are assumed to be applicable to determining the maximum second order inelastic moment ( $M_{r2-P}$ ) when flexural stiffness reduction factor  $\tau_{MN}$  are incorporated within the calculation of the elastic critical buckling load in the form of reduction factors. This analytical expression depends upon several factors but most importantly, depends on the ability of performing nonlinear advanced analysis. For practical purposes, it is interesting to develop an approximate expression based upon similar parameters but in which no previous advanced analysis is needed.

Analytical expressions of stiffness reduction factor  $\tau_{MN}$  for beam-columns are developed through extending the formulations that evaluate second order effects for elastic beam-columns to a new expression that covers the inelastic range. These formulations are assumed to be applicable to determine maximum second order inelastic moment ( $M_{r2-P}$ ) of beam-columns provided that flexural stiffness reduction factor  $\tau_{MN}$  is incorporated into elastic critical buckling load. After  $M_{r2-P}$  for studied beam-columns are obtained,  $\tau_{MN}$  determined by the analytical expression is subsequently calculated.

For sway-restrained beam-columns including material non-linearity, Eq. 20 defines the amplification factor  $B_{1-P}$  that evaluates  $P-\delta$  effects through incorporating  $\tau_{MN}$  into the expression that relates first and second order moment.

$$\frac{M_{r2-P}}{M_{r1}} \approx \frac{C_m}{1 - \frac{P_{e-\tau MN}}{P_{r1}}} = B_{1-P} \geq 1 \quad (20)$$

where

$$P_{e-\tau MN} = \tau_{MN} P_{e1} = \frac{\pi^2 (\tau_{MN} EI)}{l^2} \quad (21)$$

where  $C_m$  is equivalent uniform moment factor.  $P_{r1}$  and  $M_{r1}$  are maximum internal first order axial force and maximum internal first order moment within the member, respectively. Rewriting Eq. 20, the analytical solution of  $\tau_{MN}$  can be expressed by Eq. 22.

$$\tau_{MN} \approx \frac{P_{r1}}{(1 - C_m \frac{M_{r1}}{M_{r2-P}})(P_{e1})} \quad (22)$$

Similarly, for sway-permitted beam-columns including material nonlinearity, Eq. 23 defines the amplification factor  $B_{2-P}$  that evaluates  $P-\Delta$  effects through incorporating  $\tau_{MN}$  into the expression that relates first and second order moment.

$$\frac{M_{r2-P}}{M_{r1}} \approx \frac{1}{1 - \frac{P_{story}}{P_{e*-story-\tau MN}}} = B_{2-P} \geq 1 \quad (23)$$

where

$$P_{e*-story-\tau MN} = \tau_{MN} R_M P_{e*-st} \quad (24)$$

where  $P_{story}$  is total vertical load transferred by the story (from Linear Elastic Analysis);  $P_{e*-story}$  is elastic critical buckling (sway mode) strength of the story. Rewriting Eq.(23),  $\tau_{MN}$  for sway-permitted inelastic beam-columns can be expressed by

$$\tau_{MN} \approx \frac{P_{story}}{(1 - \frac{M_{r1}}{M_{r2-P}})(R_M P_{e*-story})} \quad (25)$$



$\tau_{MN}$  determined by Eq.(22) and Eq.(25) accounts for influence of member out-of-straightness, residual stresses and spread of plasticity, provided that the maximum second order inelastic moment ( $M_{r2-P}$ ) in these equations are obtained from an analysis that includes corresponding out-of-straightness, residual stresses and material non-linearity. Analytical expressions (22) and (25) are thoroughly validated with a set of examples in isolated members as well as with structural sub-assemblages presented in Shen and Chacón (2020<sup>a</sup>).

The aim of developing expression of  $\tau_{MN}$  is to apply a second-order elastic analysis with stiffness reduction to stability design of frames. Although  $\tau_{MN}$  determined by the two analytical expressions (Eq. 22 and 25) proves accurate, it cannot be applied directly to the design of frames, since the maximum internal second order inelastic moment ( $M_{r2-P}$ ) in the two analytical expressions is unknown. Similarly, to the method for carbon steel (White et al. 2016, Kucukler et al. 2014, Kucukler et al. 2016), flexural stiffness reduction factors for beam-columns can be determined by a function that includes the most relevant variables without the need of knowing  $M_{r2-P}$  in advance. The variables in the proposed approximate expression are: first order maximum axial force ( $P_{r1}$ ), first order maximum bending moment ( $M_{r1}$ ), equivalent uniform moment factor ( $C_m$ ), cross-section shape factor ( $W_{el}/W_{pl}$ ), second order effects factor ( $B_{2-E}$ ), column flexural stiffness reduction factor  $\tau_N$  ( $\tau_N$  depends on the independent variable  $P_{r1}$ ), beam flexural stiffness reduction factor  $\tau_M$  ( $\tau_M$  depends on the independent variable  $M_{r1}$  and material properties ( $E$ ,  $f_y$ , and  $n$ )).

The approximate expression of  $\tau_{MN}$  is developed by fitting variables to the analytical expressions determined by Eq. 22 and Eq. 25. The fitting process is carried out in Matlab (2017). Since analytical solution of  $\tau_{MN}$  accounts for member out-of-straightness of 0.001, residual stresses and spread of plasticity, these factors are consequently included in the approximate expression of  $\tau_{MN}$ .

The approximate expression of  $\tau_{MN}$  is given by the set of equations (26)-(30). It is based on the numerical study of stainless steel beam-columns with a wide range of cross-sections, length, material properties, and boundary conditions. Stochastic uncertainty in material strength and stiffness is not considered here. Reliability analysis are still needed for validating resistance factors  $\phi_c$  and  $\phi_b$  in beam-column interaction design equations.

$$\tau_{MN} = \gamma \Omega_M \tau_N \tau_M \left[ 1 - \left( \frac{P_{r1}}{P_y} \right)^{0.9} \left( C_m \frac{M_{r1}}{M_p} \right)^{\frac{W_{el}}{W_{pl}}} \right] \quad (26)$$

$$0.8 \leq \gamma = 2(B_{2-E} - 0.6) < 1 \quad \text{for } 1 \leq B_{2-E} < 1.1 \quad (27)$$

$$\gamma = 1 \quad \text{for } 1.1 \leq B_{2-E} \quad (28)$$

$$\Omega_M = 1 \quad \text{for } 0 \leq \frac{M_{r1}}{M_p} < 0.4 \quad (29)$$

$$\Omega_M = \left( 0.6 + \frac{M_{r1}}{M_p} \right)^{1.4} \quad \text{for } 0.4 \leq \frac{M_{r1}}{M_p} \leq 1 \quad (30)$$

It should be noted that, for sway-restrained beam-columns, the factor  $B_{2-E}$  is taken as 1.0. Other remarks are worth pinpointing:

- $B_{2-E} < 1.1$  means the increase of internal forces and moments due to P- $\Delta$  effects and together with P- $\delta$  effects may be no more than 10%.
- For the cases of  $1 \leq B_{2-E} < 1.1$ , when  $M_{r1}$  and  $P_{r1}$  are close to 0, the upper bound for  $\tau_{MN}$  would be  $\gamma \cdot \tau_N$  and  $\gamma \cdot \tau_M$ , respectively.
- For the cases of  $1.1 \leq B_{2-E}$ , when  $M_{r1}$  and  $P_{r1}$  are close to 0, the asymptotic upper bound of  $\tau_{MN}$  is  $\tau_N$  and  $\tau_M$ , respectively.
- When  $\gamma=1$  and  $M_{r1}/M_p \leq 0.4$ , Eq.(26) has the similar formation to beam-column stiffness reduction expression proposed by Kucukler et.al (2014).

As an example, a 3D plot for the case of sway-restrained beam-column with cross-section 150x100x8 ( $n=6$ ,  $f_y=350\text{MPa}$ ,  $E=200\text{GPa}$ ) and sway-permitted beam-column with cross-section 150x100x10 ( $n=7$ ,  $f_y=450\text{MPa}$ ,  $E=190\text{GPa}$ ) is shown in Fig. 3. For the former,  $B_{2-E}$  is assumed to be equal to 1.0 ( $\gamma=0.8$ ) and  $C_m$  is assumed to be equal to 1.0 (subjected to a pair of equal but opposite end moments). For the latter,  $B_{2-E}$  is assumed to be higher than 1.1 ( $\gamma=1$ ) and  $C_m=0.6$  (subjected to only one end moment).

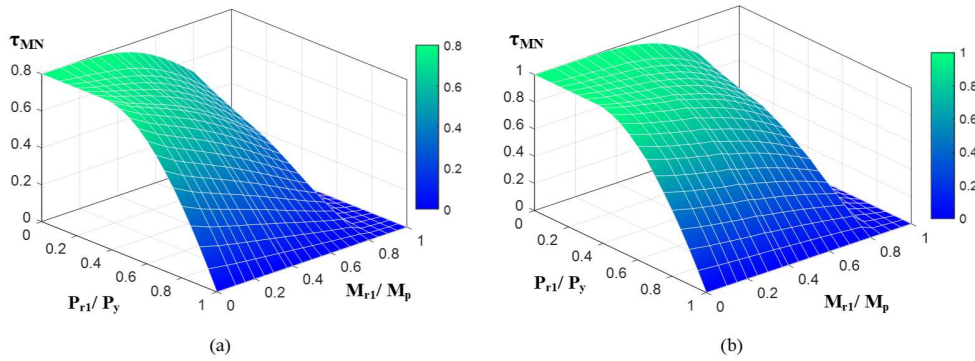


Figure 3. 3D plot of  $\tau_{MN}$ : (a) sway-restrained beam-column with cross-section 150x100x8 (b) sway-permitted beam-column with cross-section cross-section 150x150x10

Similar to the above approach, local buckling effects and the influence of initial localized imperfection on beam-columns are taken into consideration by reducing the resistance of the gross section through the strength reduction factor  $\rho$ . The extended  $\tau_{MN-\rho}$  formulation is given by Eq. 31

$$\tau_{MN-\rho} = \gamma \Omega_M \tau_{N-\rho} \tau_{M-\rho} \left[ 1 - \left( \frac{P_{r1}}{\rho P_y} \right)^{0.9} \left( C_m \frac{M_{r1}}{\rho M_p} \right)^{\frac{W_{el}}{W_{pl}}} \right] \quad (31)$$

$$0.8 \leq \gamma = 2(B_{2-E} - 0.6) < 1 \text{ for } 1 \leq B_{2-E} < 1.1 \quad (32)$$

$$\gamma = 1 \text{ for } 1.1 \leq B_{2-E} \quad (33)$$

$$\Omega_M = 1 \text{ for } 0 \leq \frac{M_{r1}}{\rho M_p} < 0.4 \quad (34)$$

$$\Omega_M = \left( 0.6 + \frac{M_{r1}}{\rho M_p} \right)^{1.4} \text{ for } 0.4 \leq \frac{M_{r1}}{\rho M_p} \leq 1 \quad (35)$$

$\tau_{N-p}$  and  $\tau_{M-p}$  in Eq.(31) are calculated based on strength reduction factor for compression ( $\rho$ -column) and strength reduction factor for bending ( $\rho$ -beam), respectively. Since flexural stiffness reduction for beam-columns was expected to be the combination of flexural stiffness reduction under compression and that under bending,  $\rho$ -column and  $\rho$ -beam ought to be used to reduce axial compression resistances and bending moment, respectively. Nevertheless, preliminary finite element analysis of some beam-columns showed that, compared to using corresponding  $\rho$ -column and  $\rho$ -beam, the adoption of the  $\min \{\rho\text{-column}, \rho\text{-beam}\}$  to reduce resistance of the gross section gave more accurate results. For the flexural stiffness reduction formulation, the influence of local buckling reduction and the interaction of axial compression and bending may be more accurately captured by adopting minimum of strength reduction factors to reduce resistance of the gross section.

For Eq. 32 and Eq. 33, the factor  $B_{2-E}$  evaluates P- $\Delta$  effects and together with P- $\delta$  effects on sway-permitted elastic beam-columns. For sway-restrained beam-columns,  $B_{2-E}$  is equal to 1. For sway-permitted beam-columns,  $B_{2-E}$  is given by Eq. 36.

$$\frac{1}{1 - \frac{P_{story}}{R_M P_{e*-story}}} = B_{2-E} \geq 1 \quad (36)$$

$$P_{e*-story} = \frac{F_H h}{\Delta} \quad (37)$$

$$R_M = 1 - 0.15 \frac{P_{mf}}{P_{story}} \quad (38)$$

where  $P_{story}$  is total vertical load transferred by the story ( $P_{story} = \sum P_{r1}$ );  $P_{e*-story}$  is elastic critical buckling (sway mode) strength of the story;  $F_H$  and  $\Delta$  are first order total story shear force and relative story drift due to  $F_H$ , respectively;  $h$  is storey height; the factor  $R_M$ , accounts for P- $\delta$  effects on the overall response of the structure,  $0.85 \leq R_M \leq 1$ ;  $P_{mf}$  is total vertical load in columns of the story that are part of moment frames.  $R_M=0.85$  for isolated sway-permitted element.

## 5. Case studies

The accuracy of 2<sup>nd</sup>-order elastic analysis with the approximately determined  $\tau_{MN}$  (denoted by 2E- $\tau_{MN}$ ) is verified for three statically indeterminate frames (compact sections). Moreover, the proposed method is compared against the direct analysis method (DM). In implementing DM, the reduced flexural stiffness  $0.8\tau_N$  is adopted. The predicted results of 2E- $\tau_{MN}$  and DM are compared against those determined by 2<sup>nd</sup>-order inelastic analysis. Two-bay two-storey frames with pinned end and a two-bay five-storey frame with fixed end, are studied. All beam-to-column joints of the studied frames are rigid. The geometry of the studied frames are shown in Fig.4, where the frames shown in (a), (b), and (c) are referred to as Frame-2X2-G, Frame-2X2-GW and Frame-2X5-GW, respectively. Members of the two-bay two-storey frames have varied cross-sections, while all members of Frame-2X5-GW have the same cross- 250x150x10. The use of the same cross-section for all members is intended to obtain widely dispersed flexural stiffness reduction factor  $\tau_{MN}$ . All beams and columns for the studied frames bend about major axis. The details of design load combinations and basic material parameters are provided in Table 1 and the set of exemplary frames is illustrated in Fig. 4.

Table. 1 Details of the studied frames

Frame	Load combination	Cross-section	E(GPa)	$f_y$ (MPa)	n
Frame-2X2-G	$1.2D_n + 1.6L_n$	Varied	200	400	7
Frame-2X2-GW	$1.2D_n + 0.5L_n + 1.6W_n$	Varied	200	400	7
Frame-2X5-GW	$1.2D_n + 0.5L_n + 1.6W_n$	250x150x10	190	450	7

For the two-bay two-storey frames, two types of load combinations are considered: (a) Gravity load combination  $1.2D_n + 1.6L_n$ , in which  $D_n$  and  $L_n$  denote nominal dead (gravity) load and nominal live (gravity) load, respectively, and the typical nominal live-to-dead load ratio  $L_n/D_n = 1.5$ . (b) Combination of wind load and gravity load  $1.2D_n + 0.5L_n + 1.6W_n$ , in which  $W_n$  denotes nominal wind load; live-to-dead load ratio  $L_n/D_n = 1.0$ , and wind-to-gravity load ratio  $W_n/(L_n + D_n) = 0.1$ . For the 2x5 frame, one load case (wind load and gravity load  $1.2D_n + 0.5L_n + 1.6W_n$ ) is considered. For all the frames, the combined load applied on the top-storey is half of that applied on other storeys.

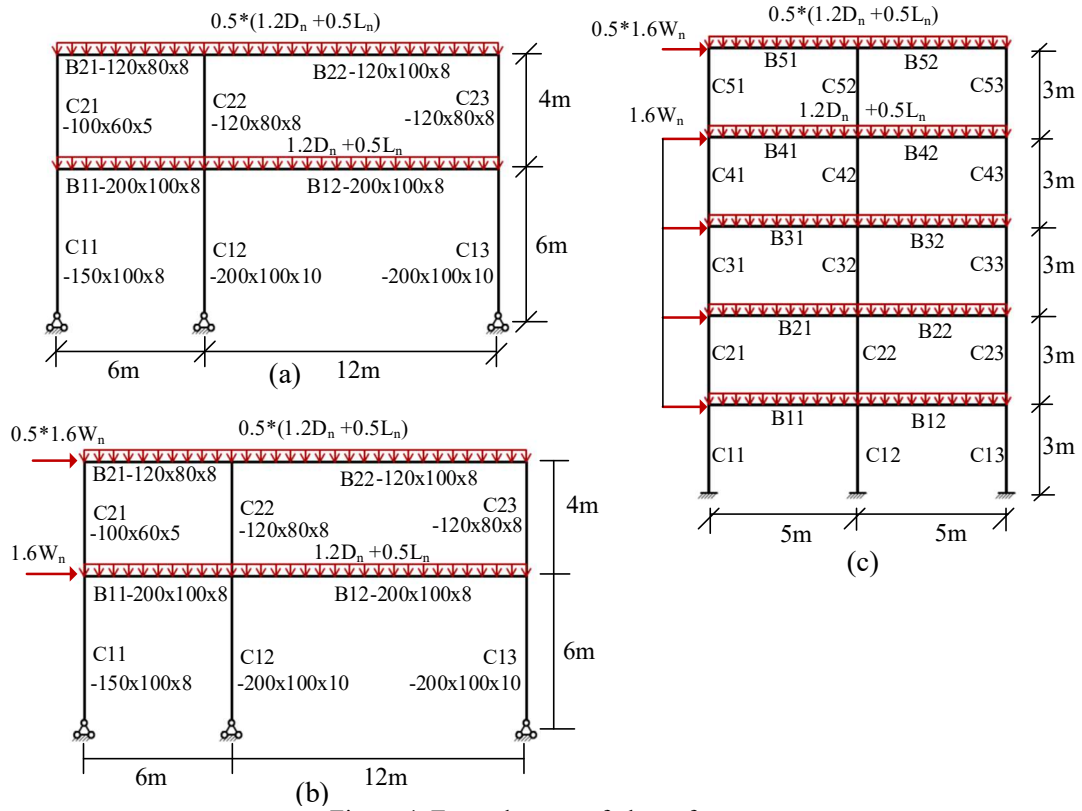


Figure 4. Exemplary set of planar frames

The procedure of implementing 2<sup>nd</sup>-order elastic analysis with  $\tau_{MN}$  ( $2E-\tau_{MN}$ ) and direct analysis method (DM) with a verification using advanced fully nonlinear analysis can be summarized with a set of steps as follows:

- The design load is defined. Given an assumed factored load, a 2<sup>nd</sup>-order inelastic analysis is conducted. The applied load is defined as a design load when the Demand-Capacity ratio ( $R_c$ ) of the critical member is equal to 1.0.

- A linear elastic analysis is performed under the design load to obtain  $P_{r1}$ ,  $M_{r1}$ ,  $P_{\text{story}}$ , and  $P_{e^*-\text{story}}$ . Then  $\tau_N$ ,  $\tau_M$ ,  $C_m$ ,  $R_M$ , and  $B_{2-E}$  are calculated according to related equations. The approximate flexural stiffness reduction factor  $\tau_{MN}$  determined by Eq. 26 is subsequently calculated.
- A  $2E-\tau_{MN}$  (as well as DM) analysis is conducted under the design load.  $2E-\tau_{MN}$  and DM are conducted to obtain the maximum internal second order forces and moments, and Demand-Capacity ratios of the members. In implementing DM, the reduced flexural stiffness  $0.8\tau_N$  is adopted.
- The 2<sup>nd</sup>-order inelastic analysis is conducted by assuming out-of-plumbness of 0.002 and out-of-straightness of 0.001 are introduced. Residual stresses are considered through modified stress-strain curves. For  $2E-\tau_{MN}$  and DM, since the influence of out-of-straightness of 0.001 and residual stresses are included in the flexural stiffness reduction factor ( $\tau_{MN}$  for  $2E-\tau_{MN}$ ;  $0.8\tau_N$  for DM), only out-of-plumbness of 0.002 is introduced to the frame models.

Results are presented for the example 2x5 GW in Fig. 5 in which the horizontal axis represents specific member in the frame (for example, 1 corresponds to C11, and 25 corresponds to B52);  $P_{r2}$ ,  $M_{r2}$  and  $R_c$  determined by 2<sup>nd</sup>-order elastic analysis with  $\tau_{MN}$  (denoted by  $2E-\tau_{MN}$ ) and DM are compared against those determined by the benchmark. For a member, maximum internal second order axial force  $P_{r2}$ , maximum internal second order moment  $M_{r2}$  and demand-capacity ratio  $R_c$  determined by 2<sup>nd</sup>-order inelastic analysis are denoted by  $P_{r2-2P}$ ,  $M_{r2-2P}$  and  $R_{c-2P}$ , respectively. For this frame, the maximum value of  $B_{2-E}$  is 1.32, and the critical member is C12.

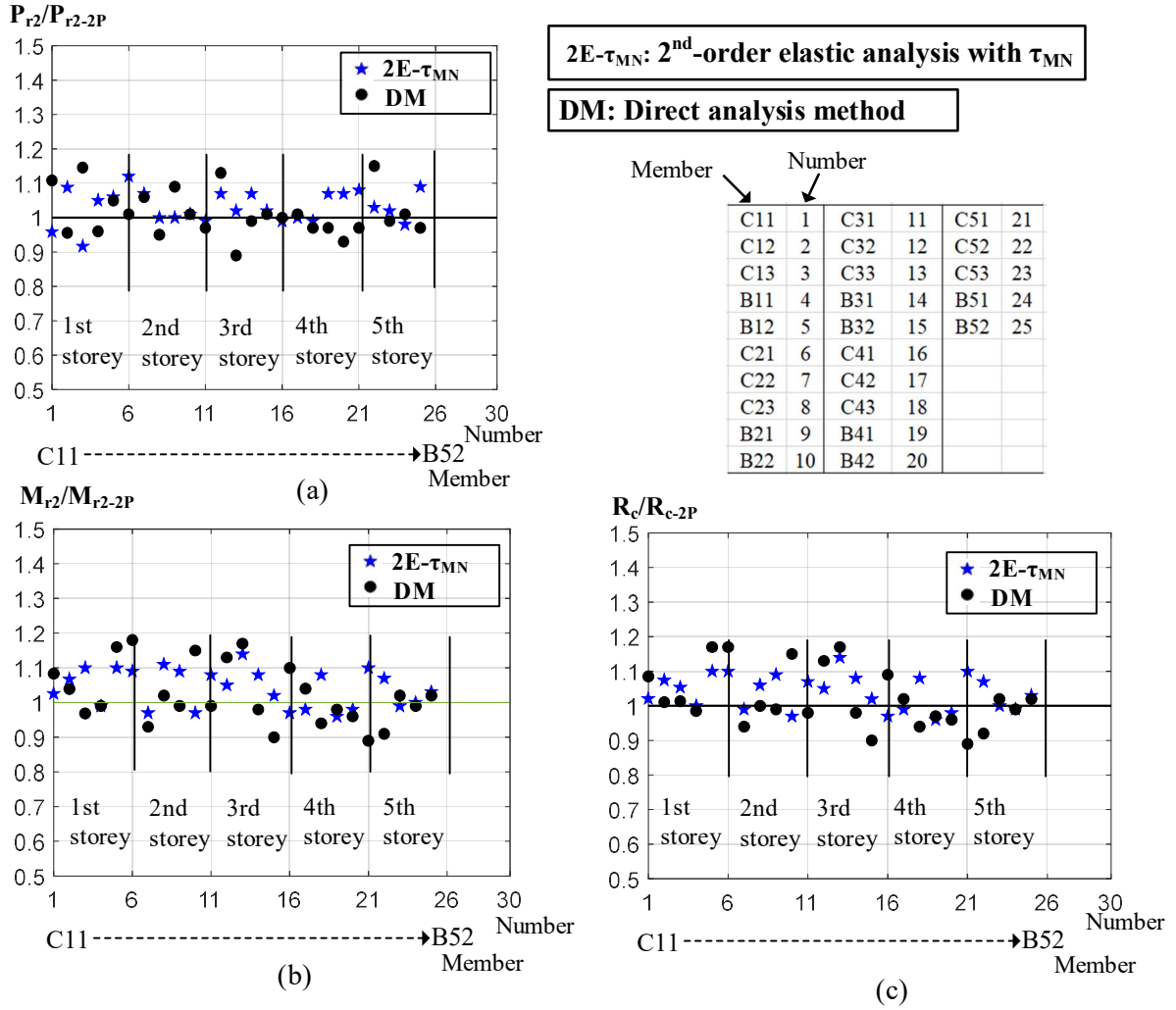


Figure 5. Comparison of the predicted results determined by different methods: (a) maximum internal second order axial force  $P_{r2}$  (b) maximum internal second order moment  $M_{r2}$  (c) demand-capacity ratio  $R_c$

It is observed that, from the 3rd storey up to the top storey, the distribution of  $R_{c-2P}/R_{c-2P}$  (or  $R_{c-2P}/R_{c-2P}$ ) is in very close agreement with the distribution of  $M_{r2-2P}/M_{r2-2P}$  (or  $M_{r2-2P}/M_{r2-2P}$ ). This is because the ratio of axial force to cross-section yield strength is small for the columns in these storeys, and thus  $R_c$  is dominated by  $M_{r2}$ .

It is observed that, compared to DM, the predicted results of 2<sup>nd</sup>-order elastic analysis with  $\tau_{MN}$  (2E- $\tau_{MN}$ ) have lower deviation from the predicted results of 2<sup>nd</sup>-order inelastic analysis. It indicates that 2E- $\tau_{MN}$  provides improved estimation for the studied frame. This is because  $\tau_{MN}$  (determined by the analytical expression) can more accurately capture stiffness reduction owing to material non-linearity, and well capture additional second order effects due to material non-linearity. For the critical member (C12), both 2<sup>nd</sup>-order elastic analysis with  $\tau_{MN}$  (2E- $\tau_{MN}$ ) and DM provide accurate and safe predictions. Nevertheless, DM produces large errors for a few of other members. The maximum error of overestimation of  $R_{c-2P}$  is within 13% for 2E- $\tau_{MN}$  and 20% for DM.

It is found that, for most members, the value of  $M_{r2-\tau_{MN}}/M_{r2-2P}$  and  $R_c-\tau_{MN}/R_c-2P$  is larger than 1. This may be explained that  $\tau_{MN}$  determined by the approximate expression is conservative. The conservative stiffness reduction produces more deformations, which in turn results in increased second order effects (P- $\Delta$  and P- $\delta$ ) and subsequently increased internal bending moment and Demand-capacity ratio.

The accuracy of the extended beam-column flexural stiffness reduction factor  $\tau_{MN-\rho}$  (in conjunction with 2<sup>nd</sup>-order elastic analysis) for in-plane stainless steel beam-columns with non-compact and slender sections is also evaluated but in this case, with simply supported beam-columns and cantilever beam-columns.

Simply supported beam-columns, with different cross-sections and material properties are shown in Table 2. These elements are subjected to combined axial load (P) and varied moments ( $M_1$ ,  $M_2$ ) at the member ends. The applied P is factored load,  $M_2=e*P$ ; e ranges from 1 to 150 ( e=[0,10,30,50,80,100,150]) and the unit of e is mm;  $|M_2| \geq |M_1|$ . The applied end moments are varied for different cross-sections: a pair of equal but opposite end moments for cross-section 120x80x2, one end moment for cross-section 200x100x3, and a pair of identical end moments for cross-section 250x150x5.

Cantilever beam-columns, with different cross-sections and material properties (also shown in Table 2), are subjected to combined axial load (P) and horizontal load (iP) at the cantilever end, where the applied load P is factored load, and  $i=[0, 0.05, 0.1, 0.15, 0.2, 0.25, 0.3]$ .

Table.2 Basic material parameters and cross-sections of the studied beam-columns

Beam-column		Cross-section	L(mm)	E(GPa)	$f_y$ (MPa)	n	$W_{pl}/W_{el}$
Simply supported	a	120x80x2	2000	200	350	6	1.19
	b	200x100x3	2500	175	400	8	1.22
	c	250x150x5	3000	190	450	7	1.20
Cantilever	a	120x80x1.5	2000	200	350	6	1.19
	b	200x200x3	2500	175	300	7	1.14

For conciseness, only the predicted strength curves for simply supported beam-columns are shown in Fig.6. The strength curves determined by 2<sup>nd</sup>-order elastic analysis with  $\tau_{MN-\rho}$  (denoted by 2E- $\tau_{MN-\rho}$ ) using beam elements are compared against those determined by a 2<sup>nd</sup>-order inelastic analysis using shell elements.  $P_n$  and  $M_n$  are the nominal compressive strength of the column and nominal flexural strength of the beam, respectively.  $P_u$  and  $M_u$  predicted by different methods are normalized by  $P_n$  and  $M_n$ , respectively. It is observed that the results predicted by 2<sup>nd</sup>-order elastic analysis with  $\tau_{MN-\rho}$  using beam elements are in close agreement with those determined by 2<sup>nd</sup>-order inelastic analysis using shell elements. For most of the studied beam-columns, the difference between the predicted results of 2<sup>nd</sup>-order elastic analysis with  $\tau_{MN-\rho}$  and those determined by shells mainly occurs in the intermediate part of the interaction curves ( $P_u/P_n$  versus  $M_u/M_n$ ). It may result from either the incorporated strength reduction factor  $\rho$  or the amplitude of introduced maximum initial localized imperfection ( $\omega_{max}$ ) in implementing shell analysis. It is concluded that, besides capturing the influence of spread of plasticity, the extended flexural stiffness reduction factor  $\tau_{MN-\rho}$  can also capture local buckling effects.

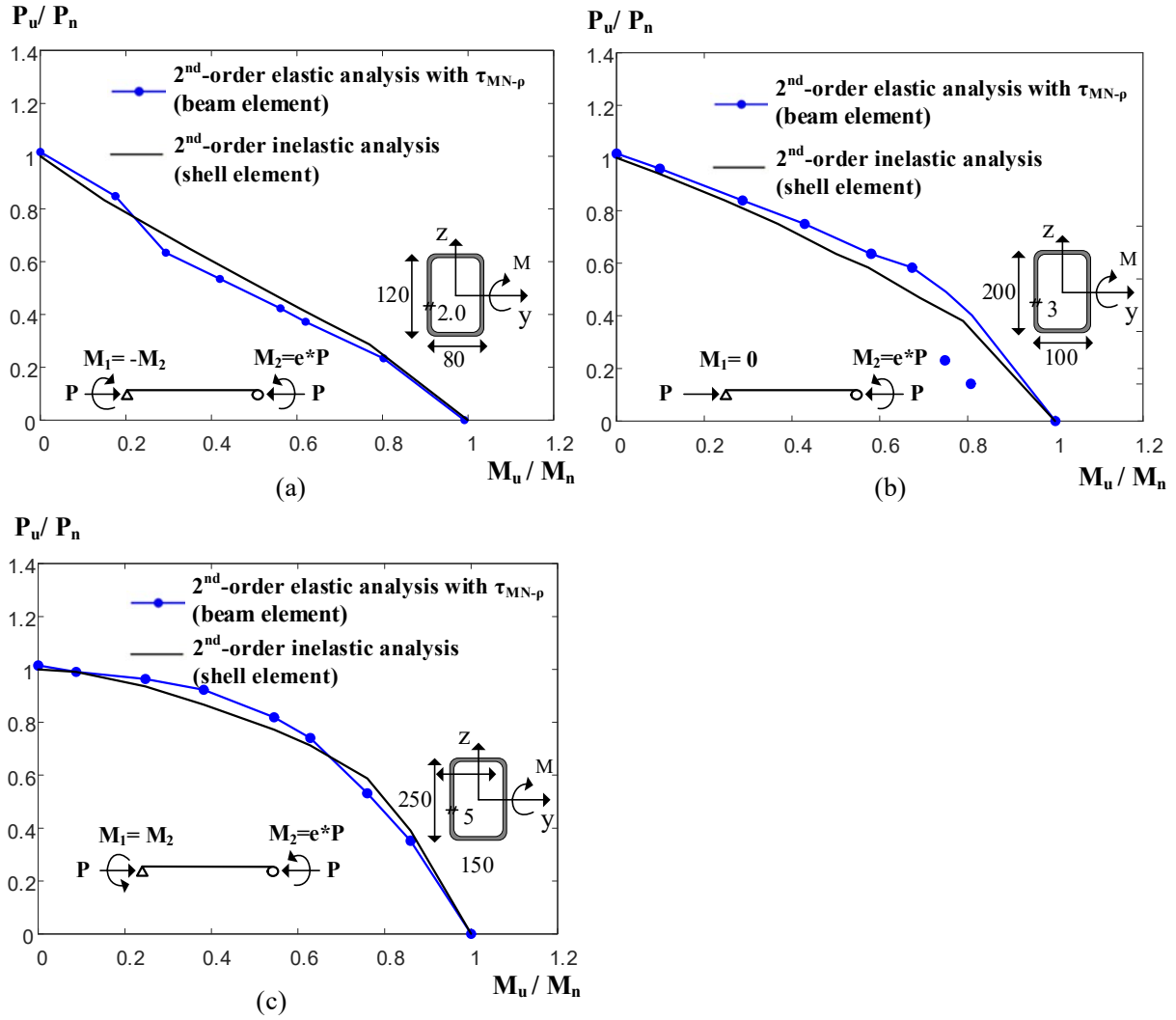


Figure 6. Verification of the approximate solutions for  $\tau_{MN-p}$

## 6. Conclusions

In this paper, flexural stiffness reduction factor for applying geometrically non-linear analysis to in-plane stability design of stainless steel multi-storey regular frames are proposed. The proposed beam-column flexural stiffness reduction factor accounts for the deleterious influence of spread of plasticity, structural imperfections (residual stresses) and member geometrical imperfections. The proposed formulation is valid for both compact and slender sections with the corresponding use of an additional strength reduction factor. The formulation is developed by means of two different methodologies: an analytical expression and an approximate expression. The accuracy of both proposals is determined through comparisons of the maximum bending moments within members determined by 2<sup>nd</sup>-order elastic analysis coupled with the proposed reduction factor and, results obtained from a fully nonlinear analysis that accounts for both geometrical and material nonlinearity (including structural and geometrical imperfections). It is observed that predicted results are in very close agreement with those established as a benchmark. When analyzing the results obtained for stainless steel frames using the Direct Analysis Method (DM) with no



modifications, the proposed approach provides improved estimations. One reason is the proposed  $\tau_{MN}$  can more accurately capture stiffness reduction resulted from material non-linearity and well capture additional second order effects due to material nonlinearity. Nonetheless, it should be mentioned that all the studied frames have not significant capacity for load redistribution. The proposed approach may be very conservative for frames that significantly benefit from load redistribution and strain hardening after the formation of the first plastic hinge. Furthermore, the applicability of the proposed approach for large redundant structural systems that have complex interactions between members should be assessed.

## Acknowledgments

The authors acknowledge the financial support provided by the Project BIA2016-75678-R, AEI/FEDER, UE “Comportamiento estructural de pórticos de acero inoxidable. Seguridad frente a acciones accidentales de sismo y fuego”, funded from the MINECO (Spain).

## References

- ANSI/AISC 360-05 (2005). “Specification for Structural Steel Buildings”, American Institute of Steel Construction, Chicago.
- ANSI/AISC 360-10 (2010). “Specification for Structural Steel Buildings”, American Institute of Steel Construction, Chicago.
- ANSI/AISC 360-16 (2016). “Specification for Structural Steel Buildings”, American Institute of Steel Construction, Chicago.
- Arrayago I., Real E., Gardner L. (2015). “Description of stress–strain curves for stainless steel alloys”. *Materials & Design*. 87 540–552.
- Arrayago I., González-de-León I., Real E., Mirambell, E. (2020). “Tests on stainless steel frames. Part I: Preliminary tests and experimental set-up”. *Thin-Walled Structures*. 157 1-14. 107500.
- Arrayago I., González-de-León I., Real E., Mirambell, E. (2020). “Tests on stainless steel frames. Part II: Results and analysis”. *Thin-Walled Structures*. 157 1-16. 107006
- Baddoo N. (2008). “Stainless steel in construction: a review of research, applications, challenges and opportunities”. *Journal of Constructional Steel Research*. 64 (11) 1199–1206.
- Baddoo N. (2013). “Design Guide 27: Structural Stainless Steel”. American Institute of Steel Construction, Chicago.
- Baddoo, N., Francis P. (2014). “Development of design rules in the AISC Design Guide for structural stainless steel”. *Thin-Walled Structures*, 83 200-208.
- Becque J., Rasmussen K.J.R. (2009). “Experimental investigation of the interaction of local and overall buckling of stainless steel I-columns”. *Journal of Structural Engineering*, 135(11) 1340-1348.
- Chacón, R., Claire, F., de Coss, O. (2020). “Development of VR/AR applications for experimental tests of beams, columns and frames”. *Journal of Computing in Civil Engineering*. 34 (5) 1-14. 05020003
- Chacón, R., Puig-Polo, C., Real, E. (2021). “TLS measurements of initial imperfections of steel frames for structural analysis within BIM-enabled platforms”. *Automation in Construction*. 125. 103618
- Design Manual for Structural Stainless steel-4th Edition. SCI Publication,
- Gardner L., Nethercot D.A. (2004). “Experiments on stainless steel hollow sections—Part 1: Material and cross-sectional behavior”. *Journal of Constructional Steel Research*. 60 1291–1318.
- Gardner L. (2019). Stability and design of stainless steel structures—Review and outlook”. *Thin-Walled Structures*. 141 208-216.
- Kim S.E, Chen W.F. (1999). “Design guide for steel frames using advanced analysis program”. *Engineering Structures* 21 352–364.
- Kucukler, M., Gardner L., Macorini L. (2014). “A stiffness reduction method for the in-plane design of structural steel elements”. *Engineering Structures* 73 72–84
- Kucukler M., Gardner L., Macorini L. (2016). “Development and assessment of a practical stiffness reduction method for the in-plane design of steel frames”. *Journal of Constructional Steel Research*, 126 187–200.
- Kucukler M., Gardner L. (2018). “Design of laterally restrained web-tapered steel structures through a stiffness reduction method”. *Journal of Constructional Steel Research*. 141, 63-76.
- Kucukler M., Gardner L. (2019<sup>a</sup>). “Design of web-tapered steel beams against lateral-torsional buckling through a stiffness reduction method”. *Engineering Structures*. 190, 246-261.

- Kucukler M., Gardner L. (2019<sup>b</sup>). “Design of hot-finished tubular steel members using a stiffness reduction method”. *Journal of Constructional Steel Research*. 160 340-358.
- Matlab (2017). Mathworks. <https://www.mathworks.com/>
- Mirambell E., Real E. (2000). “On the calculation of deflections in structural stainless steel beams: an experimental and numerical investigation”. *Journal of Constructional Steel Research* 54 (1) 109-133.
- Real E., Mirambell E. (2005). “Flexural behaviour of stainless steel beams”, *Engineering Structures* 27 1465–1475.
- Rossi B. (2014). “Discussion on the use of stainless steel in constructions in view of sustainability”. *Thin-Walled Structures*. 83 182-189
- Shen Y.F., Chacón. (2019). “Effect of uncertainty in localized imperfection on the ultimate compressive strength of cold-formed stainless steel hollow sections”. *Applied Sciences*. 9(18) 3827
- Shen Y.F., Chacón R. (2020<sup>a</sup>). “Geometrically non-linear analysis with stiffness reduction for the stability design of stainless steel structures: Application to members and planar frames”. *Thin-Walled Structures*. 148 1-19. 106581
- Shen Y.F., Chacón R. (2020<sup>b</sup>). “Flexural stiffness reduction for stainless steel SHS and RHS members prone to local buckling”. *Thin-Walled Structures*. 155 1-15. 106939
- Surovek-Maleck A.E., White D.W. (2004<sup>a</sup>). “Alternative approaches for elastic analysis and design of steel frames. I: Overview”. *Journal of Structural Engineering ASCE* 130 (8) 1186–1196.
- Surovek-Maleck A.E., White D.W. (2004<sup>b</sup>). “Alternative approaches for elastic analysis and design of steel frames. II: verification studies”. *Journal of Structural Engineering ASCE* 130 (8) 1197–1205
- Walport F., Gardner L., Real E., Arrayago I., Nethercot D. (2019). “Effects of material nonlinearity on the global analysis and stability of stainless steel frames”. *Journal of Constructional Steel Research*. 152 173–182.
- White D.W., Jeong W.Y., Toga O. (2016). “Comprehensive Stability Design of Planar Steel Members and Framing Systems via Inelastic Buckling Analysis”. *International Journal of Steel Structures*. 16(4) 1029-1042.
- White D., Surovek A.E., Alemdar B.N., Chang C., Kim Y.D., Kuchenbecker G (2006). “Stability analysis and design of steel building frames using the 2005 AISC Specification”, *Steel Structures* 6 71-91.
- Ziemian R.D., McGuire W. (2002). Modified Tangent Modulus Approach, A Contribution to Plastic Hinge Analysis, *Journal of Structural Engineering, ASCE*, 128(10) 1301-1307.
- Zubydan A.H. (2010). “A simplified model for inelastic second order analysis of planar frames”. *Engineering Structures*. 32(10) 3258–3268.